The Green Bank Telescope 350 MHz Drift-scan survey. I

Survey Observations and the Discovery of 13 Pulsars

Boyles, J.; Lynch, R.S.; Ransom, S.M.; Stairs, I.H.; Lorimer, D.R.; McLaughlin, M.A.; Hessels, J.W.T.; Kaspi, V.M.; Kondratiev, V.I.; Archibald, A.; Berndsen, A.; Cardoso, R.F.; Cherry, A.; Epstein, C.R.; Karako-Argaman, C.; McPhee, C.A.; Pennucci, T.; Roberts, M.S.E.; Stovall, K.; van Leeuwen, J.

[Link to publication](#)

THE GREEN BANK TELESCOPE 350 MHz DRIFT-SCAN SURVEY. I. SURVEY OBSERVATIONS AND THE DISCOVERY OF 13 PULSARS

J. Boyles[1,2], R. S. Lynch[3,4], S. M. Ransom[5], I. H. Stairs[6], D. R. Lorimer[1,14], M. A. McLaughlin[1], J. W. T. Hessels[7,8],
V. M. Kaspi[3], V. I. Kondratiev[7,9], A. Archibald[3], A. Berndsen[6], R. F. Cardoso[1], A. Cherry[6], C. R. Epstein[10],
C. Karako-Argaman[3], C. A. McPhee[6], T. Pennucci[4], M. S. E. Roberts[11], K. Stovall[12,13], and J. van Leeuwen[7,8]

[1] Department of Physics, West Virginia University, Morgantown, WV 26506, USA; jason.boyles@wku.edu
[2] Department of Physics and Astronomy, Western Kentucky University, Bowling Green, KY 42101, USA
[3] Department of Physics, McGill University, 3600 University St., Montrèal, Quebec, H3A 2T8, Canada
[4] Department of Astronomy, University of Virginia, Charlottesville, VA 22904-4325, USA
[5] National Radio Astronomy Observatory (NRAO), 520 Edgemont Road, Charlottesville, VA 22901, USA
[6] Department of Physics and Astronomy, University of British Columbia, 6224 Agricultural Road, Vancouver, British Columbia V6T 1Z1, Canada
[7] ASTRON, The Netherlands Institute for Radio Astronomy, Postbus 2, 7990 AA, Dwingeloo, The Netherlands
[8] Astronomical Institute "Anton Pannekoek," University of Amsterdam, Science Park 904, 1098 XH Amsterdam, The Netherlands
[9] Astro Space Center of the Lebedev Physical Institute, Profsoyuznaya str. 84/32, Moscow 117997, Russia
[10] Department of Astronomy, Ohio State University, 140 W. 18th Avenue, Columbus, OH 43210, USA
[11] Eureka Scientific, 2452 Delmer Street, Suite 100, Oakland, CA 94602-3017, USA
[12] Center for Advanced Radio Astronomy and Department of Physics and Astronomy, University of Texas at Brownsville, Brownsville, TX 78520, USA
[13] Department of Physics and Astronomy, University of Texas at San Antonio, San Antonio, TX 78249, USA

ABSTRACT

Over the summer of 2007, we obtained 1191 hr of "drift-scan" pulsar search observations with the Green Bank Telescope at a radio frequency of 350 MHz. Here we describe the survey setup, search procedure, and the discovery and follow-up timing of 13 pulsars. Among the new discoveries, one (PSR J1623−0841) was discovered only through its single pulses, two (PSRs J1327−0755 and J1737−0814) are millisecond pulsars, and another (PSR J2222−0137) is a mildly recycled pulsar. PSR J1327−0755 is a 2.7 ms pulsar at a dispersion measure (DM) of 27.9 pc cm^{-3} in an 8.7 day orbit with a minimum companion mass of 0.22 $M_\odot$. PSR J1737−0814 is a 4.2 ms pulsar at a DM of 55.3 pc cm^{-3} in a 79.3 day orbit with a minimum companion mass of 0.06 $M_\odot$. PSR J2222−0137 is a 32.8 ms pulsar at a very low DM of 3.27 pc cm^{-3} in a 2.4 day orbit with a minimum companion mass of 1.11 $M_\odot$. It is most likely a white-dwarf–neutron-star system or an unusual low-eccentricity double neutron star system. Ten other pulsars discovered in this survey are reported in the companion paper Lynch et al.

Key words: pulsars: general – pulsars: individual (PSR J1327−0755, PSR J1623−0841, PSR J1737−0814, PSR J1941−0121, PSR J2222−0137) – stars: neutron

Online-only material: color figures, machine-readable table

1. INTRODUCTION

Since the discovery of the first pulsar in 1967 (Hewish et al. 1968), many fascinating sources and experiments have been associated with pulsars. These include, but are not limited to, tests of general relativity (e.g., Lyne et al. 2004; Kramer et al. 2006), studies of binary evolution (e.g., Bhattacharya & van den Heuvel 1991), probes of electron density models of the interstellar medium (e.g., Cordes & Lazio 2002), constraints on the neutron star equation of state (e.g., Lattimer & Prakash 2001; Lattimer & Prakash 2007), and use in a pulsar timing array for gravitational wave detection (e.g., Hobbs et al. 2010; Demorest et al. 2013).

Searches for pulsars are very demanding, requiring both significant amounts of computational and human resources. The high time and frequency resolution needed for pulsar searches result in data rates greater than that for most astronomical projects (typically 100 GB hr^{-1} or more). Large computing clusters are needed to thoroughly search for both periodic and transient dispersed signals. After all the computer searches are completed, candidates are typically visually inspected to determine likely pulsar candidates, though automated algorithms are

becoming more widely used for sifting through large numbers of candidate signals (e.g., Eatough et al. 2010).

Pulsars are brighter at low frequencies (i.e., a few hundred MHz) but pulsar survey sensitivity is reduced by dispersion smearing, higher sky temperature, and scattering at these frequencies. Therefore, the most recent large-scale pulsar surveys like the Parkes Multibeam Pulsar Survey (PMPS; Manchester et al. 2001), High Time Resolution Universe Pulsar Survey (HTRU; Keith et al. 2010), and the Pulsar Arecibo *L*-band Feed Array Survey (Cordes et al. 2006) are conducted around 1.4 GHz. Lower frequency observations (<500 MHz) are better used to locate weak sources away from the Galactic plane where the effects of scattering, higher sky temperature, and dispersion broadening are minimized.

The National Radio Astronomy Observatory (NRAO) in Green Bank, WV, has a long history of successful searches for radio pulsars at low frequencies. Damashek et al. (1978) discovered 17 new pulsars with the 92 m (300′) transit telescope at a frequency of 400 MHz. Later, using the same telescope at a frequency of 390 MHz, Dewey et al. (1985) found 34 new long-period pulsars. However, they were not sensitive to newly discovered millisecond pulsars (MSPs; $P < 20$ ms; Backer et al. 1982). The first low-frequency survey to be sensitive to MSPs was conducted by Stokes et al. (1985) at 390 MHz. While this survey did not discover any MSPs, it did find 20 new long-period

pulsars. Sayer et al. (1997) used the 43 m (140′) telescope at Green Bank at a frequency of 370 MHz and discovered eight new pulsars, including one mildly relativistic binary pulsar. New backend hardware and higher data rates now allow frequency resolution that was previously unattainable by earlier observing systems. Most recently, a North Galactic plane survey was conducted with the Robert C. Byrd Green Bank Telescope[15] (GBT) by Hessels et al. (2008) at 350 MHz and discovered 33 new pulsars. None of these were MSPs despite the survey's sensitivity to these systems.[16]

Our survey took advantage of a unique opportunity when the GBT was immobilized for track refurbishing during the northern summer of 2007. During this time, we recorded data at a radio frequency of 350 MHz as the sky passed through the beam of the telescope. We will discuss these drift-scan observations in Section 2. In Section 3 we describe the follow-up observations and timing analysis of the new pulsars. In Section 4 we present the properties of the 13 pulsars and in Section 5 we discuss interesting individual objects. Finally, in Section 6 we present conclusions and the future survey planned in light of the results obtained in this survey. The survey sensitivity, pipeline, and the remaining new pulsars are discussed in Lynch et al. (2013, Paper II).

2. SURVEY OBSERVATIONS

The drift-scan observations occurred from 2007 May through August. The telescope was parked at a set azimuth during the track refurbishing and data were recorded while the sky drifted through the telescope's beam. The elevation of the telescope was adjusted and had a limit of >60° during the weekdays and >30° during the weekends. The azimuth was set at ∼229° for the first half of the observations and ∼192° for the second half of the observations. These azimuth restrictions allowed us to access declination (δ) ranges of $-7°.72 < \delta < 38°.43$ and $-20°.66 < \delta < 38°.43$ for azimuths of 229° and 192°, respectively. All right ascensions were available for us to observe.

We chose a frequency of 350 MHz for this survey for many reasons. First, at 350 MHz, the radio frequency interference (RFI) environment at the GBT is well known and remarkably manageable. Second, pulsars generally have very steep spectral indices (e.g., Sieber 1973) and our survey covers Galactic latitudes away from the Galactic plane, where propagation effects in the interstellar medium are generally less severe. Lastly, the GBT's beam size at 350 MHz is ∼36′, allowing us to cover a greater amount of the sky than would be possible with higher frequency receivers. The sky coverage rate (210 deg^2 day^{-1}) is faster than that achieved by the PMPS at 1.4 GHz (26 deg^2 day^{-1}; Manchester et al. 2001).

The now-retired Spigot auto-correlation spectrometer (Kaplan et al. 2005) was used for the GBT drift-scan observations. We used 50 MHz of bandwidth with 81.92 μs sampling time. For the first week of observations (MJDs 54222−54230), data were recorded with 1024 three-level auto-correlation functions which were accumulated into 16-bit registers for analysis. After that time and until the conclusion of the observations, a new 2048 three-level auto-correlation mode was used which accumulated data into 8-bit registers.

Data were recorded every night on each weekday and for 24 hr a day during the weekends. In total, 1491 hr of data were taken, amounting to 134 TB (see Table 5 in the Appendix for the observation list and Figure 1 for sky coverage area). This amounts to a sky coverage of 10,347 deg^2, of which ∼2800 went to the Pulsar Search Collaboratory (PSC; Rosen et al. 2010, 2012).[17] A source passing through the center of the beam is visible for roughly 140 s. Assuming a detection significance of 8σ, a digitization correction factor of 1.16 to account for three-level quantization of the signal, and a pulse duty cycle of 0.04 results in a survey flux density limit:

$$S_{\min} = 0.012 T_{\mathrm{sys}} \frac{\mathrm{mJy}}{\mathrm{K}}, \quad (1)$$

where T_{sys} is the total system temperature. The system temperature has two major components: the receiver temperature, which is ∼22 K, and the sky temperature. The sky temperature can vary greatly in the survey region. Far off the plane, the sky temperature is ∼30 K at 350 MHz but near the plane the sky temperature can be 200–400 K in our survey regions. For a total system temperature of 52 K, a survey sensitivity limit of 0.6 mJy is obtained. Scaling our flux density limit with an average pulsar spectral index of -1.8 (Maron et al. 2000) gives us a limit of ∼0.05 mJy at 1352 MHz, more sensitive than the mid- and high-latitude HTRU survey in the same regions, but our observations were hampered more significantly by dispersion smearing and scattering. A more detailed discussion of the survey sensitivity is presented in Paper II. Data processing was done with the PRESTO[18] software package (Ransom 2001) and the data pipeline will be presented in Paper II.

3. TIMING OBSERVATIONS AND ANALYSIS

Timing observations began in 2008 June. At that stage, nine new pulsars that had been discovered were observed. The first session was conducted at a central frequency of 350 MHz with the GBT using the Spigot backend with 50 MHz of bandwidth and 81.92 μs sampling time. With observations spread across 6 hr, this session was used to establish a very accurate period and for gridding of pulsars to find a more accurate position (Morris et al. 2002).

Most of the rest of the follow-up timing observations in the first year (2008 July–2009 May) were conducted using the Spigot backend at a central frequency of 820 MHz with 1024 channels, 50 MHz of bandwidth and 81.92 μs sampling time. All further observations (2009 June onward) were conducted using the Green Bank Ultimate Pulsar Processing Instrument (GUPPI) backend (Ransom et al. 2009). Most of the observations used a center frequency of 820 MHz with 200 MHz of bandwidth, 2048 channels, and 40.96 μs sampling time. For pulsars that had satisfactory timing solutions, the data were taken in online folding mode with 10 s integrations, while the rest were done in search mode, with the data recorded in PSRFITS format (Hotan et al. 2004).

Each search-mode data set was first subbanded, or de-dispersed at the pulsar's dispersion measure (DM) into broader frequency channels, using PRESTO. We used 16 subbands for long-period pulsars and 32 subbands for MSPs. The DM value
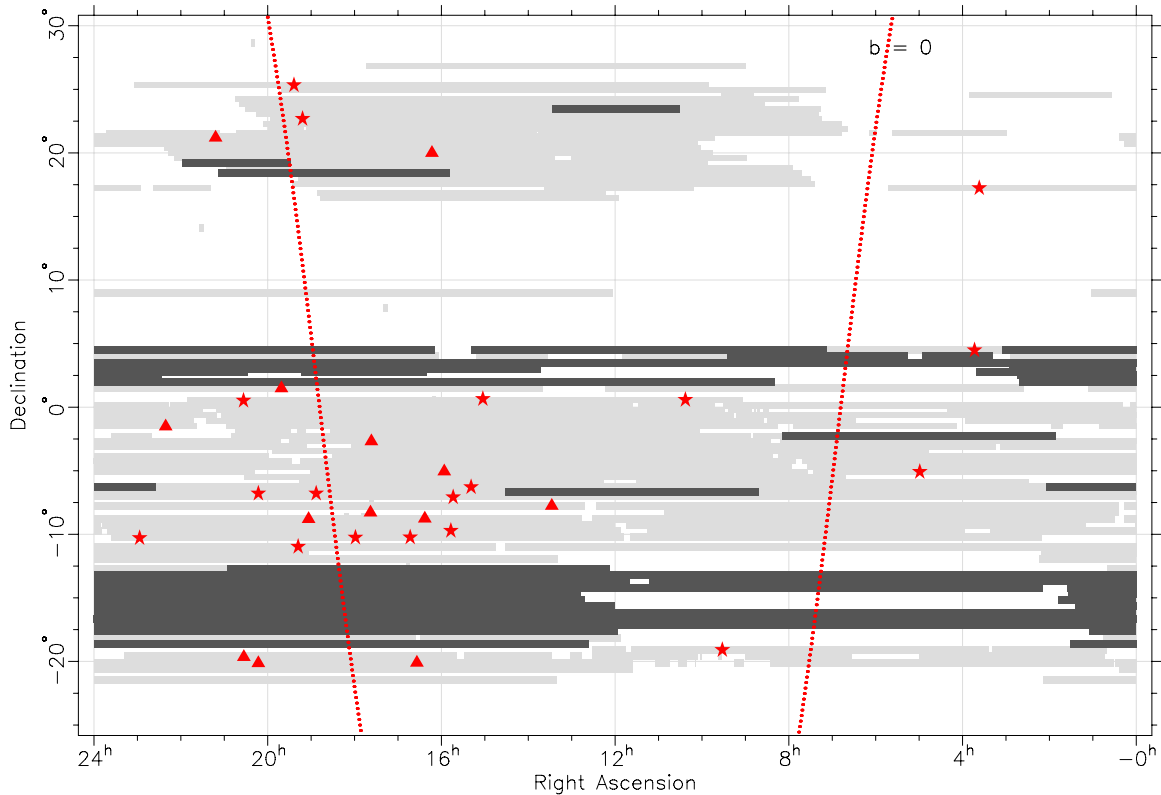

Figure 1. Sky coverage of the survey shown in right ascension and declination (J2000 coordinates). The Pulsar Search Collaboratory portion is shown in dark gray and the red dotted line shows the Galactic plane. New discoveries presented in this paper are shown as filled red triangles, while all other GBT drift-scan discoveries are shown as filled red stars.

(A color version of this figure is available in the online journal.)

used for subbanding is either the discovery value or a timing-derived value, if multi-frequency times of arrival (TOAs) had allowed fitting the DM. The online folded GUPPI data require no subbanding.

Folded pulsar profiles were created from the subbanded data using `PRESTO`; an example output plot is shown in Figure 2. These folds were done using the best available ephemeris with 128 bins for normal period pulsars or 64 bins for MSPs. Online folded GUPPI data were co-added in time and frequency and flux calibrated (described later) to form a profile using the `PSRCHIVE`[19] package with 256 pulse phase bins.

TOAs were measured from the folded profiles using the frequency-domain algorithm in `PRESTO` for all search-mode data (Taylor 1992). We measure one TOA per observation for each isolated pulsar and three per observation for each binary pulsar for better determination of binary parameters. TOAs for the online folded data were created with `PSRCHIVE` and also used the Taylor (1992) method with the same number of TOAs as the search-mode data. Templates were created by fitting multiple Gaussian functions to the summed pulse profile for each frequency and backend. From these Gaussian components, noise-free templates were created for each observing frequency with the phase of the fundamental component in the frequency domain rotated to zero.

For each pulsar, the TOAs and ephemeris files were used in `TEMPO` to carry out a standard pulsar timing analysis (see Lorimer & Kramer 2005 and references therein). The Solar System model DE405 (Standish 1998) and the time standard TT(BIPM) were used in `TEMPO`. Time delays due to using two

different backends were taken into account by placing jumps around the Spigot data, allowing a possible time offset due to each individual instrument. The result was a model for the behavior of the pulsar. The goodness of the fit was quantified by the root mean square of the difference between the model and the TOAs. The timing-derived parameters for each pulsar are listed in Tables 1–3 with doubled 1σ errors listed to provide a conservative estimate of the 68% confidence limit. The root-mean-square values are on the order of a few milliperiods. Since no systematic trends are seen in the residuals, this is interpreted as an underestimation of the individual TOA errors. As is a common practice in pulsar timing, the TOA uncertainties are scaled by a constant factor, EFAC, to bring the reduced χ^2 of each timing model to unity.

4. OTHER MEASURED PARAMETERS

4.1. 820 MHz Fluxes

Fluxes were measured using the calibration routine associated with `PSRCHIVE` with the online folded GUPPI data. On- and off-source scans of the extragalactic radio source 3C190 were used for the flux calibration. Before each observation, a 1 minute calibration scan was taken with a 25 Hz noise diode at the receiver. RFI was removed from the pulsar and calibration scan data using the `psrzap` utility from the `PSRCHIVE` package.

`PSRCHIVE` calibration was applied to the data using on- and off-flux scans, calibration scan, and pulsar data that allowed slightly different levels in the two polarizations (Hotan et al. 2004). These files were used to calculate an absolute flux conversion factor which was applied to the pulsar data. Lastly, a flux measurement was taken from the calibrated data.
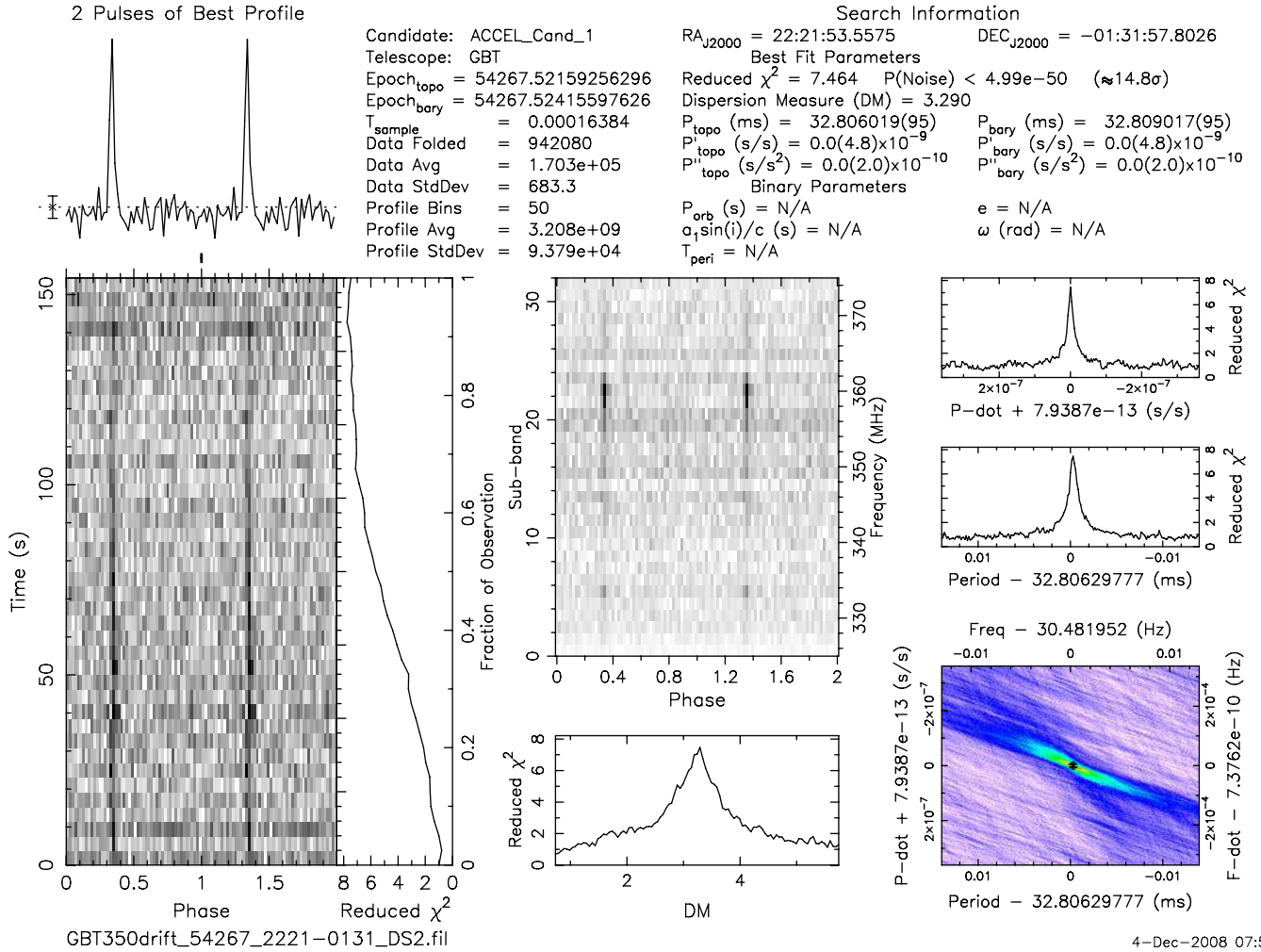
---

[19] http://psrchive.sourceforge.net/current

3

2 Pulses of Best Profile

Candidate: ACCEL_Cand_1
Telescope: GBT
Epoch$_{topo}$ = 54267.52159256296
Epoch$_{bary}$ = 54267.52415597626
T$_{sample}$ = 0.00016384
Data Folded = 942080
Data Avg   = 1.703e+05
Data StdDev = 683.3
Profile Bins = 50
Profile Avg = 3.208e+09
Profile StdDev = 9.379e+04

Search Information
RA$_{J2000}$ = 22:21:53.5575   DEC$_{J2000}$ = −01:31:57.8026
Best Fit Parameters
Reduced χ^2 = 7.464   P(Noise) < 4.99e−50   ($\approx$14.8σ)
Dispersion Measure (DM) = 3.290
P$_{topo}$ (ms) = 32.806019(95)   P$_{bary}$ (ms) = 32.809017(95)
P'$_{topo}$ (s/s) = 0.0(4.8)×10^{-9} P'$_{bary}$ (s/s) = 0.0(4.8)×10^{-9}
P''$_{topo}$ (s/s^2) = 0.0(2.0)×10^{-10} P''$_{bary}$ (s/s^2) = 0.0(2.0)×10^{-10}
Binary Parameters
P$_{orb}$ (s) = N/A   e = N/A
a$_1$sin(i)/c (s) = N/A ω (rad) = N/A
T$_{peri}$ = N/A

GBT350drift_54267_2221−0131_DS2.fil

4−Dec−2008 07:53

Figure 2. Example of the search output diagnostic plot for new discovery PSR J2222−0137. Left-hand side shows a pulse profile at the top and a plot of intensity vs. time on the bottom. Along the plot of intensity vs. time is a plot of accumulated χ^2 vs. time. The middle top plot shows observing frequency vs. pulse phase and the bottom shows χ^2 vs. DM. The right-hand side (from top to bottom) shows χ^2 vs. period, χ^2 vs. $\dot{P}$, and a χ^2 intensity plot of period-$\dot{P}$ space.

(A color version of this figure is available in the online journal.)

4.2. Rotation Measure

For pulsars with enough linearly polarized flux, rotation measures (RMs) were calculated. This includes 10 of the 13 pulsars in this sample. PSRCHIVE was used with online folded GUPPI data for producing the RMs. The method used here was similar to that presented in the recent work of Yan et al. (2011).

After the data were calibrated, we tested many different RM values from −1000 to 1000 rad m^{-2} to find the one that provided the most polarized flux. An example plot showing the results of this procedure for PSR J1941+0121 can be seen in Figure 3. A Gaussian was fit to the polarized flux versus RM and the peak of the Gaussian was taken as the best RM value. The RM values quoted for each pulsar are average values over multiple observations with the standard deviation as the uncertainty. This was done in case the ionosphere contaminated any RM measurements (see, e.g., Yan et al. 2011).

4.3. Pulse Widths at 820 MHz

Pulse widths at 50% intensity, W_{50}, were derived either by fitting a Gaussian for single peak profiles or by measuring the width across the outer edge of the profile at 50% of the peak flux for multiple component profiles. This was done for each epoch.

The W_{50} values for each epoch were averaged and the standard deviation was taken as the uncertainty.

5. DISCUSSION

Results from pulsar timing and the analysis described in Section 4 are located in Tables 1–3 for each individual pulsar and the location of each new pulsar on the $P − \dot{P}$ diagram is given in Figure 4. The DM-derived distances are from the NE2001 electron density model (Cordes & Lazio 2002). The distances have uncertainties of approximately 25%. The surface magnetic field strength, characteristic age, and spin-down luminosity are calculated using standard formulae (see, e.g., Lorimer & Kramer 2005). Pulse profiles for each pulsar can be seen in Figures 5 and 6. Some of the individual pulsars are discussed in the following subsections.

5.1. PSR J1327−0755

At the time of discovery, the narrow 350 MHz pulse width of 0.25 ms, period of 2.68 ms, and location well off the Galactic plane ($b = 54\overset{\circ}{.}3$) of PSR J1327−0755 were encouraging signs that this pulsar may be a good addition to pulsar timing arrays for the search for gravitational waves (e.g., Foster & Backer 1990).

Table 1
Timing and Derived Parameters for Newly Discovered Isolated Pulsars

Parameter	PSR J1555−0515	PSR J1612+2008
Timing parameters		
Right ascension (J2000)	15:55:40.097(16)	16:12:23.432(3)
Declination (J2000)	−05:15:57.4(5)	20:08:18.33(4)
Spin period (s)	0.97540989108(5)	0.4266459810253(12)
Period derivative (s s^{-1})	2.054(2)$\times 10^{-15}$	3.727(15)$\times 10^{-17}$
Dispersion measure (pc cm^{-3})	23.46(3)	19.544(10)
Reference epoch (MJD)	54985	54985
Span of timing data	54635–55335	54635–55335
Number of TOAs	36	41
Weighted rms residual (μs)	524	164
EFAC	3.22	1.72
Derived parameters		
Galactic longitude (deg)	3.97	35.52
Galactic latitude (deg)	34.97	43.74
Distance (kpc)	1.2	1.3
Distance from plane (kpc)	0.69	0.90
Surface magnetic field (10^{12} G)	1.4	0.13
Spin-down luminosity (10^{31} erg s^{-1})	8.8	1.9
Characteristic age (Myr)	7.4	180
820 MHz flux density (mJy)	1.2(2)	0.83(11)
W_{50} 820 MHz (ms)	12.9(3)	3.29(10)
Rotation measure (rad m^{-2})	1.3(3.0)	22(3)

Parameter	PSR J1623−0841	PSR J1633+2009
Timing parameters		
Right ascension (J2000)	16:23:42.701(19)	16:33:55.30(6)
Declination (J2000)	−08:41:36.4(9)	−20:10:09(5)
Spin period (s)	0.503014997755(14)	0.93555704483(6)
Period derivative (s s^{-1})	1.958(3)$\times 10^{-15}$	1.070(3)$\times 10^{-15}$
Dispersion measure (pc cm^{-3})	60.42(4)	48.19(6)
Reference epoch (MJD)	55079	54993
Span of timing data	54635–55522	54651–55335
Number of TOAs	36	29
Weighted rms residual (μs)	670	633
EFAC	2.17	1.62
Derived parameters		
Galactic longitude (deg)	5.77	357.63
Galactic latitude (deg)	27.37	18.33
Distance (kpc)	3.3	1.6
Distance from plane (kpc)	1.5	0.5
Surface magnetic field (10^{12} G)	1.0	1.0
Spin-down luminosity (10^{31} erg s^{-1})	63	5.0
Characteristic age (Myr)	4.1	14
820 MHz flux density (mJy)	0.42(13)	1.35(4)
W_{50} 820 MHz (ms)	11.2(3)	32.2(1.0)
Rotation measure[a] (rad m^{-2})	· · ·	−0.1(1.2)

Parameter	PSR J1735−0243	PSR J1903−0848
Timing parameters		
Right ascension (J2000)	17:35:48.1(2)	19:03:11.271(18)
Declination (J2000)	−02:43:48(5)	−08:48:57.4(8)
Spin period (s)	0.7828869765(5)	0.88732464056(4)
Period derivative (s s^{-1})	6.32(12)$\times 10^{-16}$	1.330(2)$\times 10^{-15}$
Dispersion measure (pc cm^{-3})	55.4(5)	66.99(4)
Reference epoch (MJD)	54827	54987
Span of timing data	54352–55302	54634–55339
Number of TOAs	39	51
Weighted rms residual (μs)	6532	824
EFAC	3.70	3.32
Derived parameters		
Galactic longitude (deg)	21.56	26.38
Galactic latitude (deg)	15.45	−6.60

Table 1
(Continued)

Parameter	PSR J1735−0243	PSR J1903−0848
Distance (kpc)	1.9	2.0
Distance from plane (kpc)	0.51	0.23
Surface magnetic field (10^{12} G)	0.68	1.1
Spin-down luminosity (10^{31} erg s^{-1})	4.7	7.2
Characteristic age (Myr)	21	11
820 MHz flux density (mJy)	1.3(3)	1.4(2)
W_{50} 820 MHz (ms)	102(2)	12.3(2)
Rotation measure (rad m^{-2})	28.3(1.9)	4.4(9)

Parameter	PSR J1941+0121	PSR J2012−2029
Timing parameters		
Right ascension (J2000)	19:41:16.039(16)	20:12:46.6(3)
Declination (J2000)	01:21:39.5(5)	−20:29:31(22)
Spin period (s)	0.217317451828(10)	0.54400187061(3)
Period derivative (s s^{-1})	$1.913(5) \times 10^{-16}$	$5.475(18) \times 10^{-16}$
Dispersion measure (pc cm^{-3})	52.7(7)	37.67(8)
Reference epoch (MJD)	55026	54987
Span of timing data	54712–55339	54635–55339
Number of TOAs	33	33
Weighted rms residual (μs)	555	538
EFAC	1.98	1.59
Derived parameters		
Galactic longitude (deg)	39.91	22.41
Galactic latitude (deg)	−10.43	−26.70
Distance (kpc)	2.2	1.4
Distance from plane (kpc)	0.40	0.63
Surface magnetic field (10^{12} G)	0.20	0.55
Spin-down luminosity (10^{31} erg s^{-1})	72	14
Characteristic age (Myr)	18	16
820 MHz flux density (mJy)	1.7(5)	1.00(12)
W_{50} 820 MHz (ms)	20.2(1.1)	24.2(7)
Rotation measure[b] (rad m^{-2})	−92.0(3)	⋯

Parameter	PSR J2033−1938	PSR J2111+2106
Timing parameters		
Right ascension (J2000)	20:33:55.4(2)	21:11:33.13(6)
Declination (J2000)	−19:38:59(12)	21:06:07.0(1.4)
Spin period (s)	1.28171902379(12)	3.9538529596(6)
Period derivative (s s^{-1})	$4.55(6) \times 10^{-16}$	$3.24(2) \times 10^{-15}$
Dispersion measure (pc cm^{-3})	23.47(9)	59.74(14)
Reference epoch (MJD)	54987	54987
Span of timing data	54635–55339	54635–55339
Number of TOAs	37	35
Weighted rms residual (μs)	606	2106
EFAC	2.05	2.33
Derived parameters		
Galactic longitude (deg)	25.32	69.40
Galactic latitude (deg)	−31.04	−18.20
Distance (kpc)	1.00	3.8
Distance from plane (kpc)	0.51	1.2
Surface magnetic field (10^{12} G)	0.76	3.6
Spin-down luminosity (10^{31} erg s^{-1})	0.85	0.20
Characteristic age (Myr)	44	19
820 MHz flux density (mJy)	1.13(15)	1.08(10)
W_{50} 820 MHz (ms)	32.4(3)	45(2)
Rotation measure (rad m^{-2})	−17.7(5)	−75.3(8)

Notes.
[a] PSR J1623−0841 does not have enough linearly polarized flux for an RM measurement.
[b] PSR J2012−2029 does not have enough linearly polarized flux for an RM measurement.

Table 2
Timing, Binary, and Derived Parameters for Newly Discovered Binary Pulsars

Parameter	PSR J1327−0755[a]	PSR J1737−0811
Timing parameters		
Right ascension (J2000)	13:27:57.5880(12)	17:37:47.11235(14)
Declination (J2000)	−07:55:29.80(4)	−08:11:08.887(5)
R.A. proper motion	27(18)	⋯
Decl. proper motion	95(48)	⋯
Spin period (s)	0.0026779231971205(2)	0.0041750173128551(8)
Period derivative[b] (s s^{-1})	$1.773(18)\times10^{-20}$	$7.93(8)\times10^{-21}$
Dispersion measure (pc cm^{-3})	27.91215(6)	55.311(3)
Reference epoch (MJD)	55131	54987
Span of timing data	54649–55613	54635–55339
Number of TOAs[c]	188	225
Weighted rms residual (μs)	5.5	14
EFAC	1.33	1.08
Binary parameters		
Binary model	ELL1	BT
Orbital period (days)	8.439086019(12)	79.517379(2)
Projected semimajor axis (lt-s)	6.645774(2)	9.332791(3)
Time of ascending node (MJD)	54717.3830798(7)	⋯
First Laplace-Lagrange parameter	$6(5)\times10^{-7}$	⋯
Second Laplace-Lagrange parameter	$6(7)\times10^{-7}$	⋯
Epoch of periastron (MJD)	$54718.50769778(9\times10^{-1})$	$54696.879781933(2\times10^{-1})$
Orbital eccentricity	$9(6)\times10^{-7}$	$5.38(8)\times10^{-5}$
Longitude of periastron (deg)	48(40)	49.8(9)
Mass function ($M_\odot$)	0.004425158(4)	0.0001380362(2)
Derived parameters		
Minimum companion mass[d] ($M_\odot$)	0.2219585(9)	0.0662357(3)
Galactic longitude (deg)	318.39	16.86
Galactic latitude (deg)	53.85	12.34
Distance (kpc)	1.7	1.7
Distance from plane (kpc)	1.0	0.36
Surface magnetic field[b] (10^9 G)	0.70	1.8
Spin-down luminosity[b] (10^{31} erg s^{-1})	360	430
Characteristic age[b] (Gyr)	2.4	8.3
820 MHz flux density (mJy)	0.9(2)	2.7(2)
W_{50} 820 MHz (ms)	0.131(5)	0.52(6)
Rotation measure[e] (rad m^{-2})	⋯	71.4(1.4)

Notes.
[a] Epoch of periastron, orbital eccentricity, and longitude of periastron are derived values for PSR 1327−0755.
[b] Values are not corrected for Shklovskii effect (Shklovskii 1970).
[c] Three TOAs produced per observation.
[d] Assumes a pulsar mass of 1.35 $M_\odot$.
[e] PSR J1327−0755 does not have enough linearly polarized flux for an RM measurement.

However, analysis at 820 MHz indicated that PSR J1327−0755 may not meet the standards needed for a pulsar timing arrays pulsar due to very large variations in its flux from interstellar scintillation. While ∼95% of GUPPI observations resulted in a detection, only ∼35% of Spigot observations resulted in a detection. The pulsar was typically detected in only ∼25% of the 200 MHz GUPPI bandpass, due to interstellar scintillation. The orbit has a period of 8.44 days and an eccentricity so low it has not yet been detected in our timing: $e = 9(6) \times 10^{-7}$. The projected semimajor axis of 6.65 lt-s implies a minimum companion mass of 0.22 $M_\odot$, assuming a pulsar mass of 1.35 $M_\odot$. Given the pulsar's location in the $P - \dot{P}$ diagram, the companion is very likely to be a white dwarf.

A figure of merit for the strong equivalence principle (SEP; Damour & Schaefer 1991) test is the value of P_b^2/e (Lorimer & Freire 2005). This value for PSR J1327−0755

is 7.91×10^7 days^2. This value is within the range of values for other pulsars used for SEP tests and would be a good addition to arrays of pulsar used for SEP tests (Gonzalez et al. 2011).

The composite proper motion for PSR J1327−0755 is 99 ± 23 mas yr^{-1}. This proper motion corresponds to a transverse velocity of 800 ± 200 km s^{-1} for the predicted NE2001 electron distance of 1.7 kpc. Only two recycled pulsars are known with larger values for proper motion and they are PSR J0437−4715 (Deller et al. 2009) and PSR J1231−1411 (Ransom et al. 2011). Both of these pulsars are located within 0.5 kpc of the Earth. The large proper motion most likely implies that the NE2001 model does not accurately predict distances off of the Galactic plane along this line of sight, or there are additional observational parameters that are not accounted for in PSR J1327−0755's model.

Table 3
Timing, Binary, and Derived Parameters for Newly Discovered
PSR J2222−0137

Parameter	PSR J2222−0137
Timing parameters	
Right ascension (J2000)	22:22:05.96345(8)
Declination (J2000)	−01:37:15.627(3)
Spin period (s)	0.032817859050650(5)
Period derivative (s s^{-1})	$4.74(3) \times 10^{-20}$
Second period derivative (s s^{-2})	$1.61(8) \times 10^{-27}$
Dispersion measure (pc cm^{-3})	3.27511(10)
Reference epoch (MJD)	55285
Span of timing data	54985–55585
Number of TOAs[a]	219
Weighted rms residual (μs)	8.2
Binary parameters	
Binary model	BT
Orbital period (days)	2.4457599960(5)
Projected semimajor axis (lt-s)	10.8480469(8)
Orbital eccentricity	0.00038454(14)
Longitude of periastron (deg)	119.863(14)
Time of periastron (MJD)	55284.775883844(1.0×10^{-4})
Mass function ($M_\odot$)	0.22914466(5)
Derived parameters	
Minimum companion mass[b] ($M_\odot$)	1.1169752(3)
Galactic longitude (deg)	62.02
Galactic latitude (deg)	−46.08
Distance (kpc)	0.31
Distance from plane (kpc)	0.22
Surface magnetic field (10^9 G)	1.3
Spin-down luminosity (10^{31} erg s^{-1})	5.3
Characteristic age (Gyr)	11
820 MHz flux density (mJy)	2.6(5)
W_{50} 820 MHz (ms)	0.570(5)
Rotation measure (rad m^{-2})	1.8(6)

Notes.
[a] Three TOAs produced per observation.
[b] Assumes a pulsar mass of 1.35 $M_\odot$.

5.2. PSR J1623−0841

PSR J1623−0841 was discovered only in the single-pulse search with a period of 503 ms and was labeled a rotating radio transient (McLaughlin et al. 2006). Later observations at 350 MHz with Spigot showed single pulses, but no detections were made at 820 MHz. Gridding observations were unable to localize the position better than the discovery position because of its transient nature. The final TEMPO position was 20′ away from the discovery position (outside the GBT's 820 MHz beam), and a timing solution was only attainable with the increased sensitivity of GUPPI and a dense set of observations at 350 MHz. A full discussion of PSR J1623−0841 will be presented elsewhere (J. Boyles et al., in preparation).

5.3. PSR J1737−0814

PSR J1737−0814 is a 4.18 ms binary pulsar in a low-eccentric orbit ($e = 0.000053$) with an orbital period of 79.38 days and a minimum companion mass of 0.06 $M_\odot$, assuming a pulsar mass of 1.35 $M_\odot$. Phinney (1992) predicted a relationship between orbital period and eccentricity of

$$\langle e^2 \rangle^{0.5} = 1.5 \times 10^{-4}(P_b/100 \text{ days}) \text{ for } P_b > P_{\text{crit}} \approx 25 \text{ days,}$$
(2)

Table 4
Geometric Beam Model Fit for PSR J1941+0121
Using a Complex-number RVM

Parameter	Angle (deg)	Error (deg)
ψ_0	−79	3
β	8	4
α	138	32
ϕ_0	351.7	0.8

Notes. ϕ_0 is the pulse phase of magnetic meridian, ψ_0 is position angle at ϕ_0, α is the colatitude of magnetic axis, and β is the impact parameter.

based on fluctuation dissipation theory in the second star. The orbital eccentricity for PSR J1737−0814 is about a factor of two lower than predicted by the model, but within the model's uncertainty. This indicates that the system may have followed the expected binary evolution for longer-period recycled pulsars.

In principle, the low eccentricity should make this pulsar an excellent candidate for tests for violation of the SEP (Damour & Schaefer 1991) as well as the combined Lorentz-invariance and momentum-conservation strong-field Parameterized Post-Newtonian parameter $\hat{\alpha}_3$ (Bell & Damour 1996). However, the companion mass predicted by the core-mass–orbital-period relationship (Tauris & Savonije 1999) is approximately 0.33 $M_\odot$, meaning that, unless the system inclination angle is about 15° or less (which has an a priori likelihood of less than 4%), the system may have had a different evolutionary history. Since it is best to use a set of sources that have followed the same evolutionary path for these tests (Wex 2000; Gonzalez et al. 2011), PSR J1737−0811 may not be suitable for inclusion after all. We note that PSR J1327−0755 has a minimum companion mass very close to the value predicted by the (Tauris & Savonije 1999) relation, therefore it *is* a pulsar that should be included in future editions of the ensemble tests for these parameters that would indicate a departure from General Relativity.

5.4. PSR J1941+0121

PSR J1941+0121 has the shortest period (217 ms) of the non-recycled pulsars found in this survey and about 85% of its total flux is linearly polarized. This high percentage of linearly polarized flux, along with its relatively wide pulse width ($\epsilon = 0.093$, where ϵ is the pulse width divided by pulse period), allowed us to produce a model of the pulsar's emission using the PSRCHIVE software package. A complex-value Rotating Vector Model (RVM; Radhakrishnan & Cooke 1969) was fit to the Stokes Q and Stokes U profiles, treating them as real and imaginary numbers instead of the single parameter value of position angle. Figure 7 shows the best fit of the model and Table 4 gives the model fit parameters. The model gives an impact parameter (i.e., angle between magnetic field axis and line of sight, β) of 8° ± 4° and a best-fit inclination angle (i.e., angle between rotation axis and magnetic field axis, α) of 138° ± 32°. These parameter values indicate an inner line of sight for this pulsar. The model has a χ^2 of 23.2 with 31 degrees of freedom (on-pulse phase bins minus number of fitted parameters), giving a reduced χ^2 of 0.74.

5.5. PSR J2222−0137

PSR J2222−0137 is in a low-eccentricity orbit ($e = 0.00038$) with an orbital period of 2.4 days and a projected semimajor
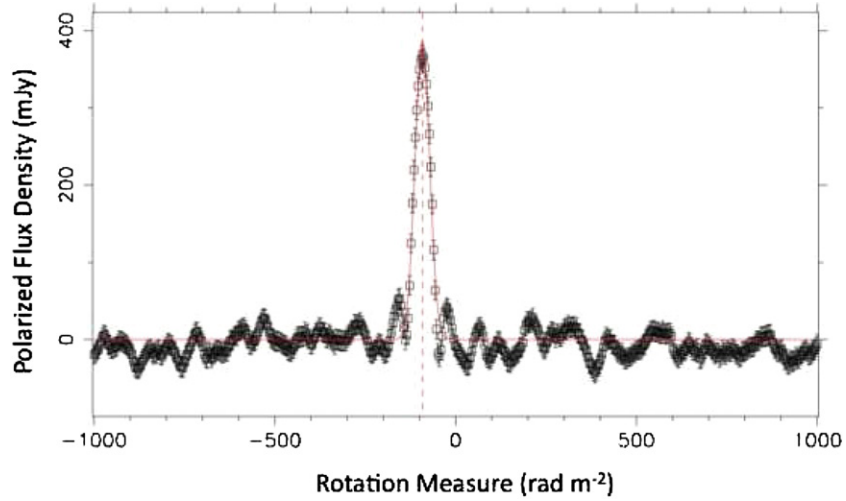
Figure 3. Example fit for RM for PSR J1941+0121. The data points are square boxes with error bars and the best-fit RM is shown by a vertical dotted line.
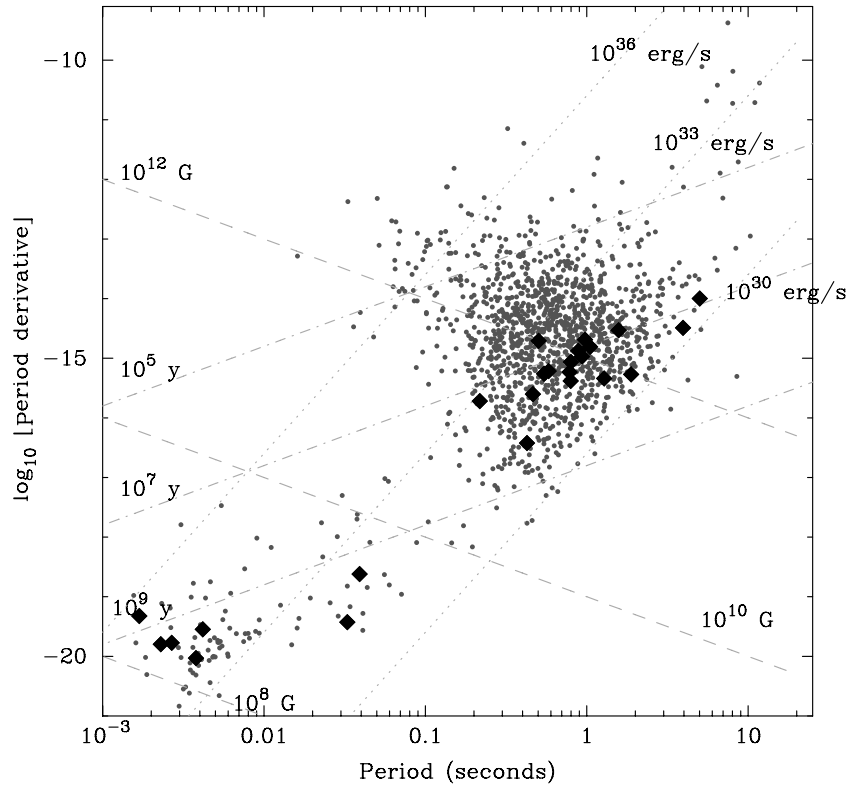(A color version of this figure is available in the online journal.)

Figure 4. $P - \dot{P}$ diagram showing the new discoveries reported in this paper and the companion paper Paper II as black diamonds. The lines on the plot show constant spin-down luminosity (dotted line), constant magnetic field (dash line), and constant characteristic age (dot-dashed line). The pulsar population is taken from the ATNF pulsar catalog (Manchester et al. 2005, http://www.atnf.csiro.au/research/pulsar/psrcat/).

axis of 10.8 lt-s. The orbital parameters imply a mass function of $0.229\,M_{\odot}$. Assuming a pulsar mass of $1.35\,M_{\odot}$ results in a minimum companion mass of $1.11\,M_{\odot}$. The spin period of 33 ms, the binary parameters, and the lack of a large $\dot{P}$ indicate that this pulsar is a partially recycled pulsar. Based on these parameters and what is known about other binary pulsars, this object is most likely a member of the so-called "intermediate-mass binary pulsars" (e.g., Camilo et al. 2001) in which the companion star is a CO white dwarf. It is also possible, though less likely, given the low orbital eccentricity, that PSR J2222−0137 is a member of a double neutron star binary

system. About a dozen of the early follow-up observations of PSR J2222−0137 have been searched for a second pulsar without success with a minimum detectable flux density of $11\,\mu$Jy at 1400 MHz.

The presence of a second period derivative suggests that there are unmodeled effects in the residuals. An unmodeled Shapiro delay signal (as the pulsar's emission passes through the gravitational potential of the companion) and no measured proper motion could be contributing to the second period derivative. We are not yet able to fit for this delay, but with a minimum companion mass of $1.11\,M_{\odot}$ and narrow pulse
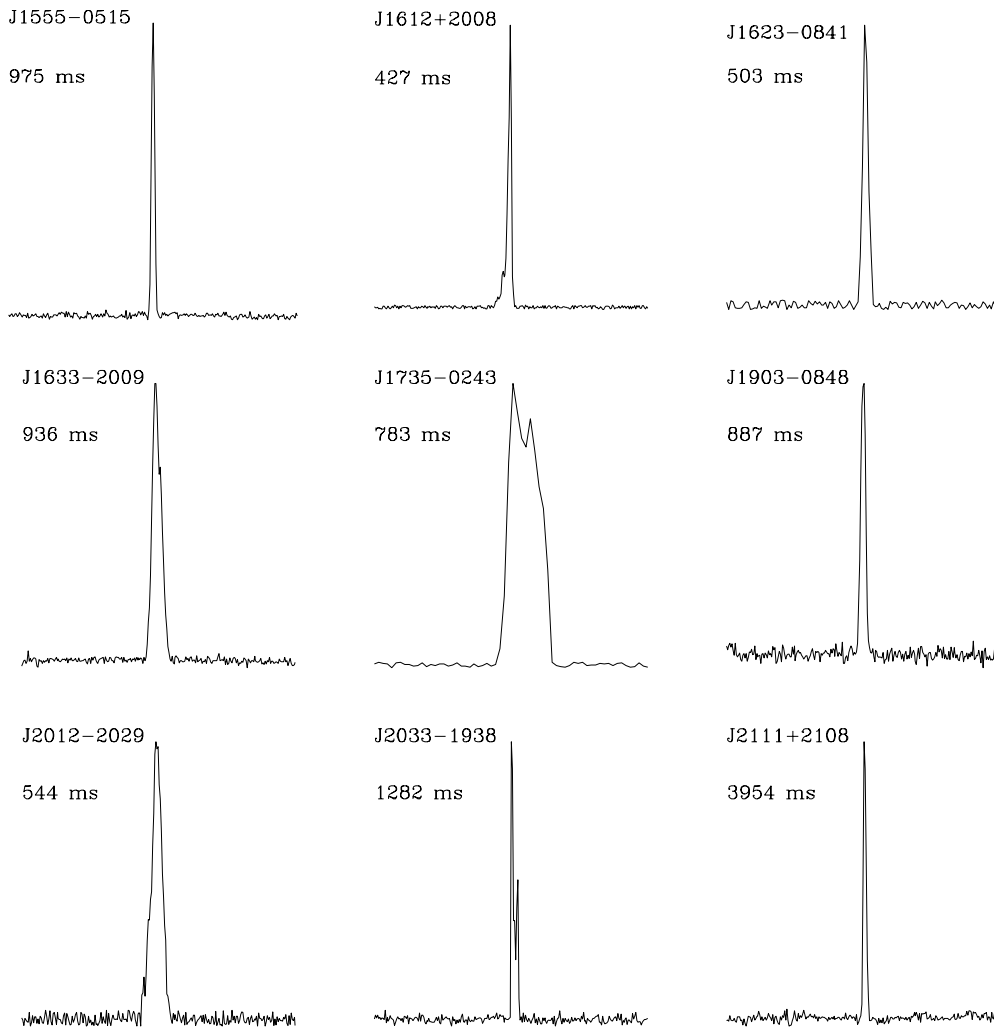
Figure 5. Profiles at 820 MHz for nine newly discovered pulsars created from multi-epoch data using the GUPPI backend. Spin periods are listed.

duty cycle of 0.017, it should be measurable, leading to the companion mass and orbital inclination. Due to the possible effects of unmodeled variables and a reduced χ^2 of 13.3, no EFAC is included for PSR J2222−0137's timing model, given in Table 4. An updated Shapiro delay and Very Long Baseline Array (VLBA) proper motion measurement, along with an updated timing solution, will be reported in a future publication.

Using the DM value of 3.28 pc cm^{-3}, the NE2001 electron density model predicts a distance of ∼300 pc to PSR J2222−0137 (Cordes & Lazio 2002). If correct, PSR J2222−0137 would be the second closest binary pulsar system after PSR J0437−4715, which has a DM of 2.64 pc cm^{-3} and a distance of 156 pc (Deller et al. 2009). For pulsars located this close to us, a large window of multi-wavelength observations opens up. These will include VLBA observations to measure proper motion and parallax, optical observations to search for an optical companion, X-ray observations to look for blackbody emission from the neutron star, and gamma-ray observations to look for higher magnetosphere emission. These observations will be reported in a future publication.

6. CONCLUSIONS AND FUTURE WORK

The 350 MHz drift-scan survey revealed many interesting pulsars with a range of physical questions that they can address. Along with PSR J2222−0137, featured in this work,

PSR J1023+0038 (Archibald et al. 2009), PSR J2256−1024 (I. H. Stairs et al., in preparation), and PSR J0348+0438 (Paper II) have been studied in greater detail. Due to the success of this survey, a new survey named the Green Bank North Celestial Cap (GBNCC) survey is underway (K. Stovall et al., in preparation). In this survey we are taking advantage of the newest pulsar instrument on the GBT, the GUPPI backend, which allows 100 MHz of bandwidth at 350 MHz. This survey will be 30%–40% more sensitive than the survey described in this paper and will be a powerful probe of the MSP population in the northern sky. The GBNCC survey will eventually cover the whole entire northern sky visible by the GBT.
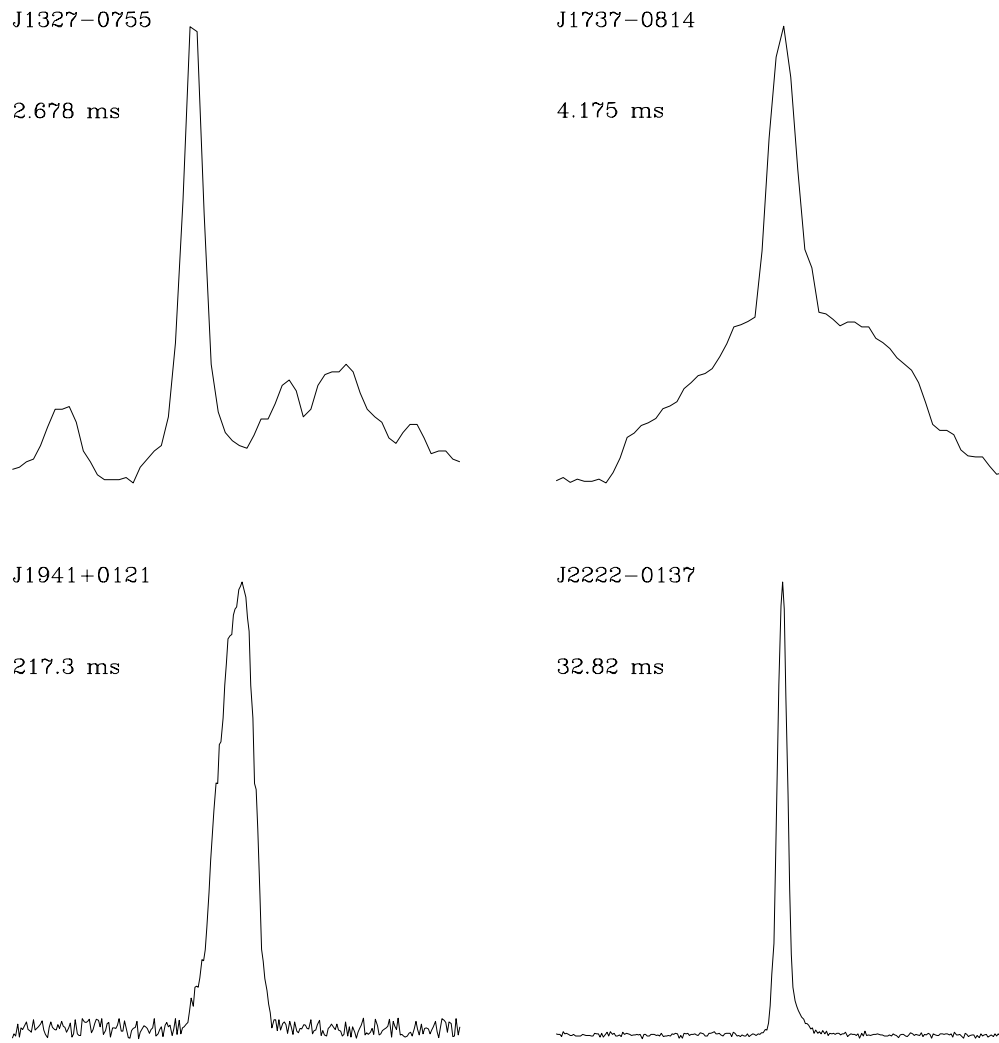
Figure 6. Profiles at 820 MHz for the remaining four newly discovered pulsars created from multi-epoch data using the GUPPI backend. The spin periods are listed.
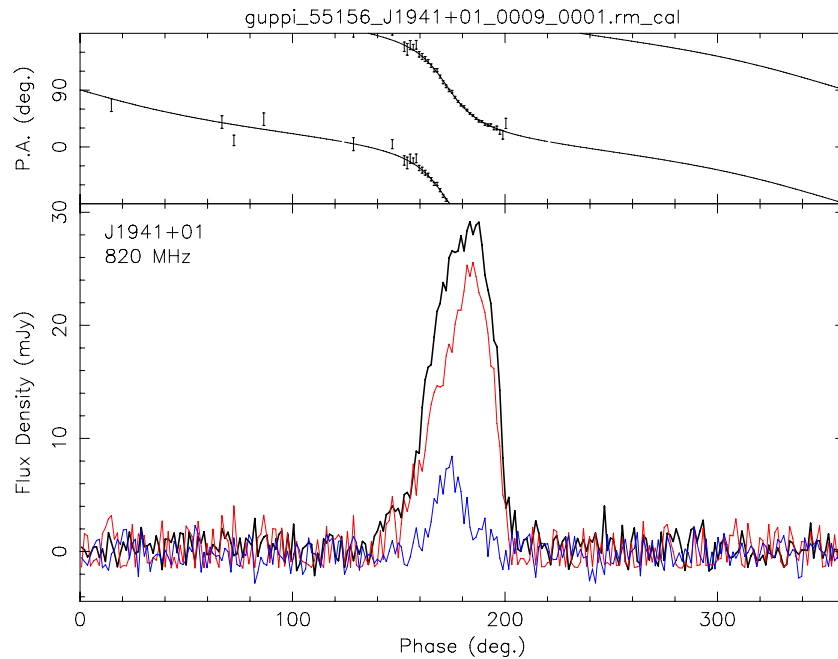

Figure 7. RVM model fit for the radio emission of PSR J1941+0121. The top plot shows parallactic angle vs. pulse phase, while the bottom plot shows integrated pulse flux density vs. pulse phase for total intensity (black line), linearly polarized flux (red line), and circularly polarized flux (blue line).

(A color version of this figure is available in the online journal.)

11

APPENDIX

Table 5 contains a list of observations taken during the drift-scan survey. These observations were conducted while the telescope was immobilized. A description of the observations is contained in the text.

Table 5
Survey of Observations

Start MJD, total time, azimuth, elevation, and number of bits stored for each survey observation

54222.171759	24640	229.240	60.0	16
54223.181169	23840	229.380	60.5	16
54224.093518	12320	229.450	61.0	16
54224.554143	4720	229.450	61.0	16
54224.621643	24320	229.450	61.0	16
54224.907592	33280	229.480	35.0	16
54225.301921	20320	229.480	35.0	16
54225.959525	43200	229.480	35.0	16
54226.500116	28800	229.480	35.5	16
54226.837373	37040	229.480	35.5	16

(This table is available in its entirety in a machine-readable form in the online journal. A portion is shown here for guidance regarding its form and content.)

REFERENCES

Archibald, A. M., Stairs, I. H., Ransom, S. M., et al. 2009, Sci, 324, 1411
Backer, D. C., Kulkarni, S. R., Heiles, C., Davis, M. M., & Goss, W. M. 1982, Natur, 300, 615
Bell, J. F., & Damour, T. 1996, CQGra, 13, 3121
Bhattacharya, D., & van den Heuvel, E. P. J. 1991, PhR, 203, 1
Camilo, F., Lyne, A. G., Manchester, R. N., et al. 2001, ApJL, 548, 187
Cordes, J. M., Freire, P. C. C., Lorimer, D. R., et al. 2006, ApJ, 637, 446
Cordes, J. M., & Lazio, T. J. W. 2002, arXiv:astro-ph/0207156v3
Damashek, M., Taylor, J. H., & Hulse, R. A. 1978, ApJL, 225, 31
Damour, T., & Schaefer, G. 1991, PhRvL, 66, 2549
Deller, A. T., Tingay, S. J., Bailes, M., & Reynolds, J. E. 2009, ApJ, 701, 1243
Demorest, P. B., Ferdman, R. D., Gonzalez, M. E., et al. 2013, ApJ, 762, 94
Dewey, R. J., Taylor, J. H., Weisberg, J. M., & Stokes, G. H. 1985, ApJL, 294, 25
Eatough, R. P., Molkenthin, N., Kramer, M., et al. 2010, MNRAS, 407, 2443
Foster, R. S., & Backer, D. C. 1990, ApJ, 361, 300
Gonzalez, M. E., Stairs, I. H., Ferdman, R. D., et al. 2011, ApJ, 743, 102
Hessels, J. W. T., Ransom, S. M., Kaspi, V. M., et al. 2008, in AIP Conf. Proc. 983, 40 Years of Pulsars: Millisecond Pulsars, Magnetars and More, ed. C. Bassa, Z. Wang, A. Cumming, & V. M. Kaspi (Melville, NY: AIP), 613
Hewish, A., Bell, S. J., Pilkington, J. D. H., Scott, P. F., & Collins, R. A. 1968, Natur, 217, 709
Hobbs, G., Archibald, A., Arzoumanian, Z., et al. 2010, CQGra, 27, 084013
Hotan, A. W., van Straten, W., & Manchester, R. N. 2004, PASA, 21, 302
Kaplan, D. L., Escoffier, R. P., Lacasse, R. J., et al. 2005, PASP, 117, 643
Keith, M. J., Jameson, A., van Straten, W., et al. 2010, MNRAS, 409, 619
Kramer, M., Stairs, I. H., Manchester, R. N., et al. 2006, Sci, 314, 97
Lattimer, J. M., & Prakash, M. 2001, ApJ, 550, 426
Lattimer, J. M., & Prakash, M. 2007, PhR, 442, 109
Lorimer, D. R., & Freire, P. C. C. 2005, in ASP Conf. Ser. 328, Binary Radio Pulsars, ed. F. A. Rasio & I. H. Stairs (San Francisco, CA: ASP), 19
Lorimer, D. R., & Kramer, M. 2005, Handbook of Pulsar Astronomy (Cambridge: Cambridge Univ. Press)
Lynch, R. S., Boyles, J., Ransom, S. M., et al. 2013, ApJ, 763, 81
Lyne, A. G., Burgay, M., Kramer, M., et al. 2004, Sci, 303, 1153
Manchester, R. N., Hobbs, G. B., Teoh, A., & Hobbs, M. 2005, AJ, 129, 1993
Manchester, R. N., Lyne, A. G., Camilo, F., et al. 2001, MNRAS, 328, 17
Maron, O., Kijak, J., Kramer, M., & Wielebinski, R. 2000, A&AS, 147, 195
McLaughlin, M. A., Lyne, A. G., Lorimer, D. R., et al. 2006, Natur, 439, 817
Morris, D. J., Hobbs, G., Lyne, A. G., et al. 2002, MNRAS, 335, 275
Phinney, E. S. 1992, RSPTA, 341, 39
Radhakrishnan, V., & Cooke, D. J. 1969, Astrophys. Lett., 3, 225
Ransom, S. M. 2001, PhD thesis, Harvard Univ.
Ransom, S. M., Demorest, P., Ford, J., et al. 2009, American Astronomical Society Meeting Abstracts, 214, 605.08
Ransom, S. M., Ray, P. S., Camilo, F., et al. 2011, ApJL, 727, 16
Rosen, R., Heatherly, S., McLaughlin, M. A., et al. 2010, AEdRv, 9, 010106
Rosen, R., Swiggum, J., McLaughlin, M. A., et al. 2012, ApJ, submitted (arXiv:1209.4108)
Sayer, R. W., Nice, D. J., & Taylor, J. H. 1997, ApJ, 474, 426
Shklovskii, I. S. 1970, SvA, 13, 562
Sieber, W. 1973, A&A, 28, 237
Standish, E. M. 1998, HiA, 11, 310
Stokes, G. H., Taylor, J. H., Welsberg, J. M., & Dewey, R. J. 1985, Natur, 317, 787
Tauris, T. M., & Savonije, G. J. 1999, A&A, 350, 928
Taylor, J. H. 1992, RSPTA, 341, 117
Wex, N. 2000, in IAU Colloq. 177: Pulsar Astronomy - 2000 and Beyond, Vol. 202, ed. M. Kramer, N. Wex, & N. Wielebinski (San Francisco, CA: ASP), 113
Yan, W. M., Manchester, R. N., Hobbs, G., et al. 2011, Ap&SS, 335, 485